



Contents lists available at ScienceDirect

Journal of Cranio-Maxillo-Facial Surgery

journal homepage: www.jcmfs.com

Accuracy of three-dimensional, paper-based models generated using a low-cost, three-dimensional printer

Raphael Olszewski^a, Piotr Szymor^{b,*}, Marcin Kozakiewicz^b

^a Oral and Maxillofacial Surgery Research Lab IREC/CHEX/OMFS, Université Catholique de Louvain, Av. Hippocrate 55, B1.55.04, B-1200 Brussels, Belgium

^b Department of Maxillofacial Surgery, Medical University of Lodz, Zeromskiego 113, 90-549 Lodz, Poland

ARTICLE INFO

Article history:

Paper received 11 June 2014

Accepted 16 July 2014

Available online xxx

Keywords:

Cone-beam computed tomography

Anatomical models

Surgical models

Maxillofacial surgery

CAD–CAM

ABSTRACT

Our study aimed to determine the accuracy of a low-cost, paper-based 3D printer by comparing a dry human mandible to its corresponding three-dimensional (3D) model using a 3D measuring arm.

One dry human mandible and its corresponding printed model were evaluated. The model was produced using DICOM data from cone beam computed tomography. The data were imported into Maxilim software, wherein automatic segmentation was performed, and the STL file was saved. These data were subsequently analysed, repaired, cut and prepared for printing with netfabb software. These prepared data were used to create a paper-based model of a mandible with an MCor Matrix 300 printer.

Seventy-six anatomical landmarks were chosen and measured 20 times on the mandible and the model using a MicroScribe G2X 3D measuring arm. The distances between all the selected landmarks were measured and compared. Only landmarks with a point inaccuracy less than 30% were used in further analyses.

The mean absolute difference for the selected 2016 measurements was 0.36 ± 0.29 mm. The mean relative difference was $1.87 \pm 3.14\%$; however, the measurement length significantly influenced the relative difference.

The accuracy of the 3D model printed using the paper-based, low-cost 3D Matrix 300 printer was acceptable. The average error was no greater than that measured with other types of 3D printers. The mean relative difference should not be considered the best way to compare studies. The point inaccuracy methodology proposed in this study may be helpful in future studies concerned with evaluating the accuracy of 3D rapid prototyping models.

© 2014 European Association for Cranio-Maxillo-Facial Surgery. Published by Elsevier Ltd. All rights reserved.

1. Introduction

Three-dimensional (3D) rapid prototyping models (RPM) are used in many clinical applications of maxillofacial surgery, including orthognathic surgery, reconstructive posttraumatic and oncological surgery, and implantology (Olszewski, 2013). There are four main RPM technologies: stereolithography, selective laser sintering, 3D impression, and fused deposition modelling. However, there are limitations in using 3D RPM on the large scale because of the cost of RPM, the cost of the 3D printer, and the cost of investment in the necessary technology. However, with the recent interest in low-cost 3D printers, the opportunity to identify a low-

cost 3D printer available for maxillofacial clinical applications has emerged. The accuracy of an RPM from a low-cost 3D printer should be evaluated to enable its use in clinical applications. Our study aimed to determine the accuracy of the low-cost, paper-based 3D Matrix 300 printer (MCor Technologies, Dunleer, Ireland) by comparing a dry human mandible (gold standard) to its corresponding 3D model printed with the Matrix 300 using a 3D measuring arm (MicroScribe G2X 3D).

2. Materials and methods

The Medical University of Lodz Ethic Committee approval was obtained for this study [RNN/248/13/KN]. Cone beam computed tomography (CBCT) (Accuitomo, Morita, Kyoto, Japan) (Primo et al., 2012) of one dry human mandible (Figs. 1–3), specimen number K3, from the anatomical collection of Hasselt University (Professor Ivo Lambrichts, Biomedical Research Institute, Laboratory of

* Corresponding author.

E-mail addresses: raphael.olszewski@uclouvain.be (R. Olszewski), piotr.szymor@gmail.com, piotr.szymor@stud.umed.lodz.pl (P. Szymor), mm_kk@toya.net.pl (M. Kozakiewicz).

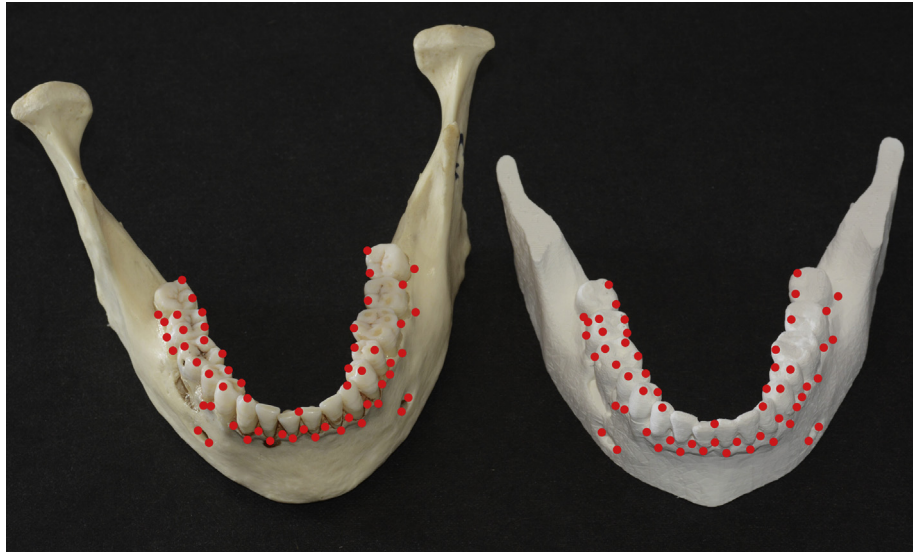


Fig. 1. Comparison of a dry human mandible with its corresponding 3D printed paper model. Anatomical landmarks are marked with dots. A detailed description is provided in [Table A1](#).

Morphology, Hasselt University, Belgium) was performed with the following parameters: 140×100 mm field of view, 90 kV, 5 mA, in Hifi mode, 0.25 mm pixel size, and 0.5 mm slice thickness.

DICOM data gathered from the CBCT were imported to Maxilim 3.2 (Medicim, Mechelen, Belgium), automatic segmentation of the mandibular bone and teeth was performed, and the STL file was saved. In the next step, the STL file was analysed, repaired, cut and prepared for printing with Netfabb software (Netfabb, Parsberg, Germany); only closed and repaired STL files are accepted by the 3D printer software.

The STL file was then imported into Slic3r 4.7 (MCor Technologies, Dunleer, Ireland), the PC-based software that controls the Matrix 300 3D printer. In this software, each imported part is analysed and cut into 0.1 mm layers that are equal to the thickness of the utilised A4 sheet of paper (Plantin, Evere, Belgium). The

prepared 2D data were sent to the Matrix 300 printer, where a tungsten blade cut a sheet of paper layer by layer according to the medical imaging data. The layers were glued together with eco-friendly adhesive (MCor Technologies, Dunleer, Ireland). The printer uses A4 80gsm paper sheets (Plantin, Evere, Belgium) and water-soluble adhesive (MCor Technologies, Dunleer, Ireland). When the printing is complete, excess paper around the printed 3D object must be removed in a process called “weeding” ([Fig. 4](#)). During this process, certain small and protruding elements, such as teeth cusps or bony edges, may be damaged. Objects in which the long axis is perpendicular to the paper layer are especially prone to such damage.

Subsequently, 76 anatomical landmarks ([Table A1](#)) were chosen on the dry mandible and on the corresponding 3D printed paper-based model ([Figs. 1–3](#)). Based on other studies ([Choi et al., 2002](#);

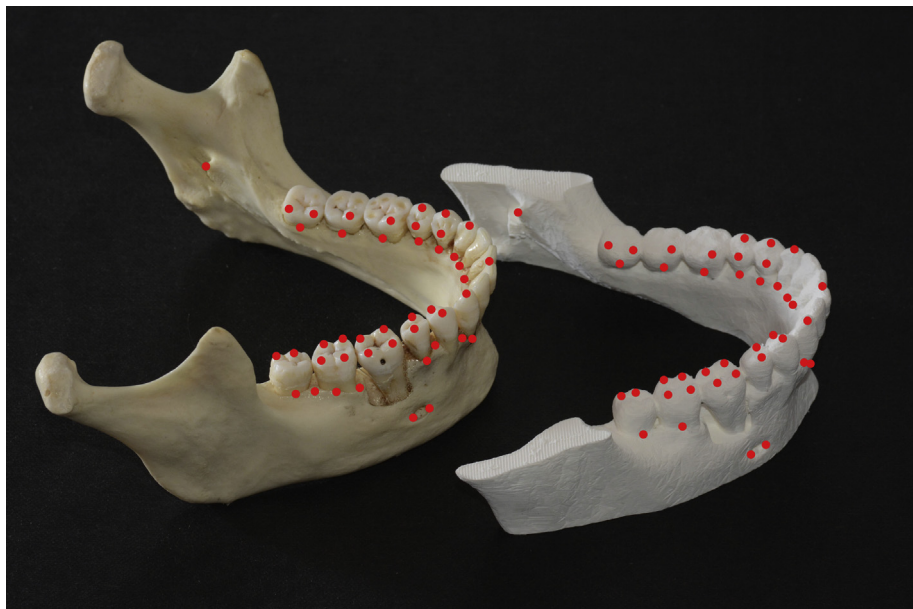


Fig. 2. Comparison of a dry human mandible with the 3D printed paper model. Anatomical landmarks are marked with dots. A detailed description is provided in [Table A1](#).

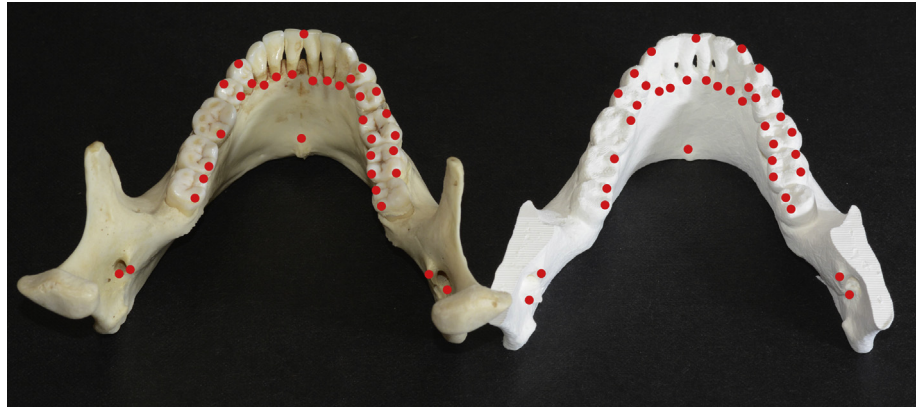


Fig. 3. Comparison of a dry human mandible with the 3D printed paper model. Anatomical landmarks are marked with dots. A detailed description is provided in Table A1.

Ibrahim et al., 2009; Primo et al., 2012; Silva et al., 2008) that compared a dry skull to a corresponding printed model, each landmark location was measured 20 times using a MicroScribe G2X 3D measuring arm (Revware Inc., Raleigh, NC, USA) and MicroScribe Utility Software v6.0.2 (Revware Inc., Raleigh, NC, USA). The Cartesian coordinates of each landmark (X, Y, and Z) were collected. Because it is nearly impossible to place the dry mandible and the printed model in exactly the same position in relation to the measuring arm, the distances between all the selected landmarks were measured and compared.

AB measured distance

$$= \sqrt{(X_A - X_B)^2 + (Y_A - Y_B)^2 + (Z_A - Z_B)^2} \text{ distance}$$

The relative and absolute differences were calculated for each of the distances based on the mean of 20 measurements with the formula proposed by Choi et al. (2002) and later repeated in other studies (Ibrahim et al., 2009; Murugesan et al., 2012; Primo et al., 2012; Silva et al., 2008).

relative difference (%)

$$= \frac{\text{skull measurement} - \text{model measurement}}{\text{skull measurement}} 100\%$$

absolute difference (mm)

$$= |\text{skull measurement} - \text{model measurement}|$$

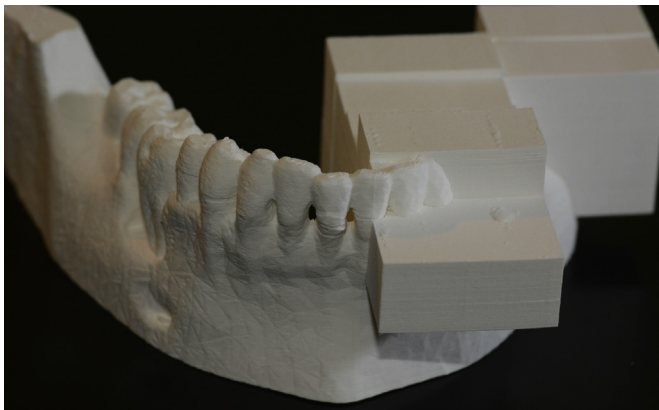


Fig. 4. 3D printed paper model of a human mandible during the weeding process.

The mean of the absolute values for the relative differences (mean dimensional error) was also calculated.

The repeatability of the measurements for the dry mandible and the 3D printed model was calculated using the formula proposed by Salmi et al. 2013. Because the number of measurements was greater than 10, the confidence factor was set to 1 in the equation.

repeatability (%)

$$= \text{confidence factor} * \text{standard deviation of measurement}$$

Because anatomical landmarks were used for the measurements, the authors proposed a method for verifying the accuracy of the anatomical landmarks represented on the model and therefore for determining which anatomical landmarks could be used in the measurements. The mean error of the MicroScribe measuring arm was calculated using a digital calliper (Mitutoyo, Chicago, USA) set for a specific distance. Next, 75 possible distances for each of 76 landmarks on the 3D printed model and the dry human mandible were calculated, for a total number of 2850 distances. The mean and standard deviation of the distances were calculated for the dry mandible and the 3D printed model based on 20 repeated measurements. The mean absolute difference for each of the 2850 measurements was calculated. Based on ISO documentation (ISO 5725-1, 1994; ISO/IEC 17025, 2005) and the Joint Committee for Guides in Metrology guide on the expression of uncertainty in measurement (Working Group 1 of the Joint Committee for Guides in Metrology (JCGM/WG 1), 2008), each pair within the 2850 total distances was defined as acceptable if the absolute difference between the pair was smaller than the sum of the standard deviation of the measurements and the previously measured mean error of the MicroScribe measuring arm (Revware Inc., Raleigh, NC, USA).

$$|\text{skull measurement} - \text{model measurement}| \leq \text{SD}_{\text{skull}} + \text{SD}_{\text{model}} + 2 * \text{MicroScribe error}$$

The number of measurements (N_{sd}) with a relative difference greater than the sum of the standard deviations and the mean error of measurement was compared with the total number of measurements (N_t) for each landmark. The result was presented as the point inaccuracy (PI) in Table A1.

$$PI(\%) = \frac{N_{sd}}{N_t} * 100\%$$

Based on the Automotive Industry Action Group standards (Automotive Industry Action Group (AIAG) et al., 2002), which state that measuring systems with more than 30% error are unacceptable, landmarks 3, 4, 5, 6, 7, 11, 53, 63, 65, 66, 69, and 76 (i.e., posterior edge of the right mental foramen, anterior edge of the right mental foramen, midline foramen, anterior edge of the left mental foramen, posterior edge of the left mental foramen, bone edge between 48 and 47, 48 mesial lingual cusp, 45 vestibular cusp, 44 lingual cusp, 43 cusp, 33 cusp, 34 vestibular cusp, and 38 distal lingual cusp) had a PI greater than 30% and were not included in further analyses. This resulted in 2016 acceptable measurements. The results were statistically analysed using Statistica 10 (StatSoft Inc., Tulsa, OK, USA) and STATGRAPHICS Centurion (STATGRAPHICS Centurion, Warrenton, Virginia, USA) with statistical significance set at $p < 0.05$.

3. Results

The mean point inaccuracy was 17.51% (Table A1). There was no statistically significant difference in the inaccuracies of bone versus tooth landmarks. The mean relative difference (%) for the 2016 measurements was $1.87 \pm 3.14\%$. The mean absolute difference was 0.36 ± 0.29 mm. However, the average Pearson correlation between the relative difference and the measurement length was $r = -0.48$ ($p < 0.05$; Fig. 5). There was no correlation between the absolute difference and the measured distance ($r = -0.063$, $p < 0.05$; Fig. 6).

The ANOVA of the mean absolute differences revealed that there was no statistically significant difference between tooth–tooth and tooth–bone measurements; however, bone–bone measurements were statistically different from the other groups (Fig. 7).

The measured repeatability was 0.48% for the dry human mandible and 0.27% for the paper-based 3D printed model.

4. Discussion

The relative difference results that were obtained from the paper-based 3D printed model of the dry mandible were similar to those obtained for 3D models created using other well-recognised 3D printing technologies, such as stereolithography, fused deposition modelling, or selective laser sintering (Choi et al., 2002; D'haese et al., 2012; Fortin et al., 2002; Ibrahim et al., 2009;

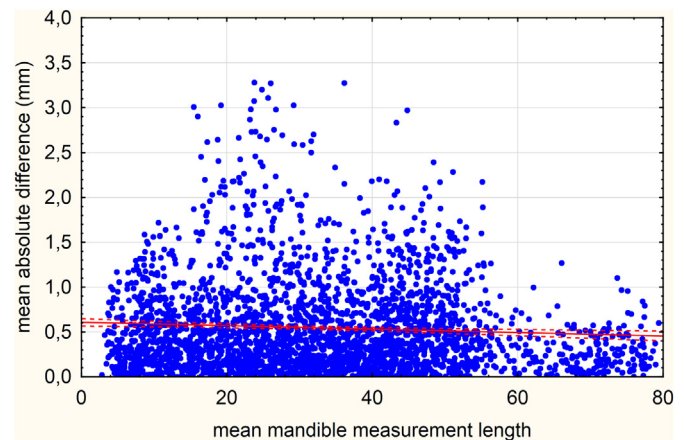


Fig. 6. Correlation between the measured distance and the mean absolute difference (%). There was no correlation between the absolute difference and the measurement length ($r = -0.063$, $p < 0.05$).

Markowska et al., 2009; Murugesan et al., 2012; Primo et al., 2012; Salmi et al., 2013; Silva et al., 2008; Taft et al., 2011). However, the average correlation between the measured distance and the relative difference and the lack of a gold standard for determining the accuracy of maxillofacial 3D printed models make comparisons between studies difficult (Fig. 5). Choosing distant measurement points may improve the accuracy of models if only the mean relative differences are compared (Nizam et al., 2006). In this study, the relative difference was 0.73% when only distances longer than 50 mm were considered (Table 1). Therefore, the authors strongly suggest not using the relative difference as the way to compare studies. However, the relative difference remains useful for studies using the same computed tomography data and measuring exactly the same landmarks because it clearly conveys the accuracy of 3D models created using different methods.

The mean absolute difference was 0.36 ± 0.29 mm, with a maximum of 1.67 mm. These values are similar to those reported in other studies measuring a 3D printed skull. Choi et al. (2002) compared a dry human skull with a stereolithographic model. The mean absolute difference was 0.62 ± 0.35 mm. Taft et al.

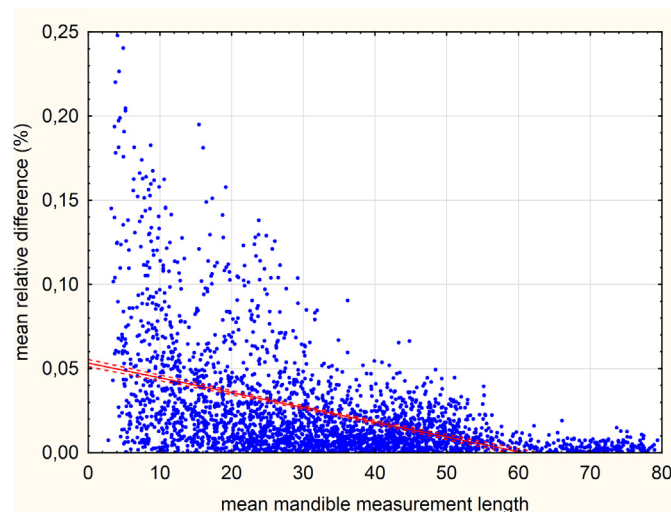


Fig. 5. Correlation between the measured distance and the mean relative difference (%). The Pearson correlation between the relative difference and the measurement length was $r = -0.48$ ($p < 0.05$).

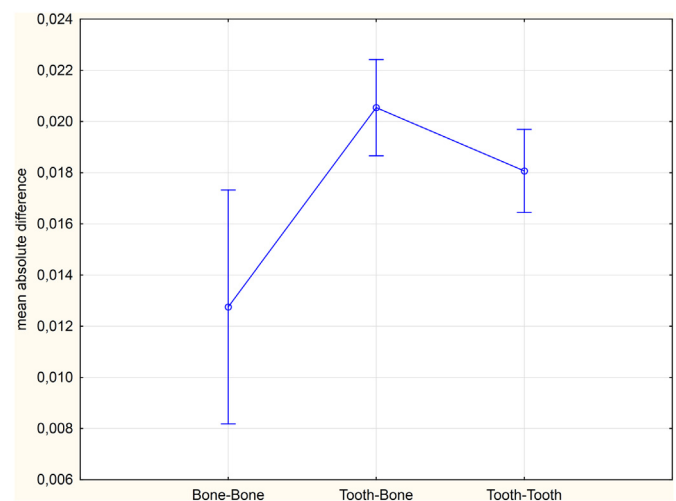


Fig. 7. ANOVA of the mean absolute difference according to the location of a point. Bone-to-bone measurements were statistically different from the other measurement groups.

Table 1

Dependence of the relative difference (%) on the measurement length. With longer measurements, the mean relative difference decreased. The accuracy can be artificially increased by using only specific long distances.

Length of measurement	Number of measurements	Mean relative difference
All measurements	2016	1.87%
>10 mm	1807	1.40%
>20 mm	1423	0.94%
>30 mm	1067	0.78%
>40 mm	676	0.71%
>50 mm	300	0.49%

(2011) obtained a mean absolute deviation of 0.608 ± 0.096 mm and reported a maximal absolute deviation of 0.703 mm in the stereolithographic skull model. Nizam et al. (2006) compared a dry human skull and a stereolithographic model and achieved a mean absolute difference of 0.23 ± 1.37 mm. Silva et al. (2008) compared selective laser sintering and 3D printing prototypes and reported a mean absolute difference of 0.89 mm for the SLS prototype and 1.07 mm for the 3DP prototype. Murugesan et al. (2012) attained much better accuracy using a PolyJet model (mean relative difference of 0.133%) compared with the 3DP models and the fused deposition models (1.67 and 1.73%, respectively). However, there are no data available on the absolute differences in this study. Salmi et al. (2013) compared SLS, PolyJet and 3DP prototypes with a 3D virtual model of a skull and reported a mean absolute difference of 0.20 ± 0.14 mm for the PolyJet model, $0.44\text{--}0.80 \pm 0.25\text{--}0.51$ mm for the 3DP model and $0.93 \pm 0.38\text{--}0.41$ mm for the SLS model. The maximal difference was 0.49 mm for the PolyJet model, 1.66 mm for the 3DP model and 1.89 for the SLS model. Ibrahim et al. (2009) compared SLS, 3DP, and PolyJet models with a dry human mandible and observed mean absolute differences of 0.90 mm, 1.44 mm and 1.23 mm, respectively. Primo et al. (2012) compared a dry human skull to a 3DP model produced with cone beam computed tomography data. The observed mean relative difference was 0.62% for the prototype obtained using multislice computed tomography, 0.74% for the prototype produced using CBCT with a 0.25 mm voxel size, and 0.82% for CBCT with a 0.40 mm voxel size. No absolute difference data were provided in this study.

The absolute difference did not correlate with the measured distance ($r = -0.063$, $p < 0.05$). This expected lack of correlation proved that the measurements were performed correctly. Furthermore, the absolute differences may be useful for comparing studies.

The differences between the dry mandible and its corresponding printed 3D model may have resulted from errors during each manufacturing step, from the acquisition of the CBCT data to human errors during the weeding and measurement steps with the 3D measuring arm. The slice thickness of the utilised CBCT scans was 0.5 mm. Primo et al. (2012) proved that this thickness provides adequate resolution for preparing a 3D printed model of a dry mandible. However, some details are irreversibly lost in a 3D printed model due to the slice thickness, the volume-averaging effect (Choi et al., 2002), and the threshold value. Additional post-processing, although performed carefully, can also introduce errors, especially when multiple software programs are used. Errors may also occur during the printing process, where the blade sometimes cuts small details, and during weeding, when residual paper is removed from the final model and small details can be lost. Ultimately, human error is a primary contributor to measurement errors (Salmi et al., 2013).

Faced with numerous potential pitfalls, the authors decided to introduce a point inaccuracy value that helps define whether the landmarks were located and measured accurately. A large

inaccuracy for certain points may be the result of all of the mentioned possible errors. Most of the landmarks that were rejected because of a high point inaccuracy were located either on the bone foramina or the teeth cusps. The possible explanations for these inaccuracies are associated with difficulties in finding the exact same spot on the dry human mandible and the 3D printed model because of either severely abraded cusps, lack of detail, errors during the weeding process and human error. The repeatability was 0.48% for the dry human mandible and 0.27% for the 3D printed model. The observed difference is probably associated with minimal sliding of a tip on the measuring arm on bone and teeth. Salmi et al. (2013) reported measurement accuracies of 0.08–0.12% with the help of a robotic arm.

The statistically lower differences that were observed in the measured bone-to-bone distances compared with the other measurement groups are difficult to explain. One possible explanation is that there is minimal movement of teeth in their sockets in the dry human mandible. There was no such movement in the 3D printed paper model. Pressure from the measuring arm could minimally shift the teeth in relationship to the bone in the dry human mandible, resulting in the observed difference.

Certain details were lost during the weeding process. Furthermore, printing and weeding the model are time consuming. For the presented mandible, printing took 16 h, and weeding took 5 h.

The cost of a 3D paper-based model is less than that of a model made of photopolymerisable resin because of the cost of paper (500 sheets for 7.5 euros, 200 sheets are required for one 3D mandible model). The weeding process was time-consuming for this particular model because of the 3D tooth reconstruction. However, only handwork and pliers are necessary for weeding the extra paper around the 3D model; more complex parts and processes are required for post-processing stereolithography or 3D printed models (cyanoacrylate glue baths). Finally, 3D paper models are fully biodegradable, whereas other commonly used 3D printed parts are not.

5. Conclusions

The accuracy of 3D models printed with a paper-based, low-cost Matrix 300 3D printer was acceptable. The average error of 0.36 ± 0.29 mm was no greater than that measured for other types of 3D printers. A gold standard should be set for comparing different methods of 3D printing. The mean relative difference is not the best value for comparing studies because measurement length has a significant influence on the results. The proposed point inaccuracy methodology may be useful for future studies concerned with checking the accuracy of a 3D RPM. Further studies should test the cytotoxicity and sterilisation of 3D paper-based RPMs from a Matrix 300 printer to ensure they are safe to use in the operating field.

Conflicts of interest statement

None declared.

Acknowledgements

We would like to thank Fondation saint Luc-Fonds Hervé Rey-chler 2013, Cliniques universitaires saint Luc, Brussels, Belgium for grant which allowed Pr Raphael Olszewski to purchase Mcor Matrix 300 three-dimensional printer for the OMFS Lab (SSS/IREC/CHEX).

Study was supported by Medical University of Lodz, grant no 503/5-061-02/503-01.

Appendix A

Table A1

List of the utilised anatomical landmarks. Rejected landmarks with a point inaccuracy greater than 30% are italicised.

No	Name of the landmark	Location	Point inaccuracy
1	Right mandibular foramen	Bone	5.33%
2	Right lingula of mandible	Bone	2.67%
3	<i>Posterior edge of mental foramen right</i>	<i>Bone</i>	<i>61.33%</i>
4	<i>Anterior edge of mental foramen right</i>	<i>Bone</i>	<i>69.33%</i>
5	<i>Midline foramen</i>	<i>Bone</i>	<i>61.33%</i>
6	<i>Anterior edge of mental foramen left</i>	<i>Bone</i>	<i>77.33%</i>
7	<i>Posterior edge of mental foramen left</i>	<i>Bone</i>	<i>46.67%</i>
8	Left lingula of mandible	Bone	4.00%
9	Left mandibular foramen	Bone	5.33%
10	Vestibular point on tooth 48	Tooth	8.00%
11	<i>Bone edge between 48 and 47</i>	<i>Bone</i>	<i>37.33%</i>
12	Vestibular point on tooth 47	Tooth	17.33%
13	Bone edge between 47 and 46	Bone	18.67%
14	Vestibular point on tooth 45	Tooth	12.00%
15	Bone edge between 45 and 44	Bone	9.33%
16	Bone edge between 44 and 43	Bone	8.00%
17	Vestibular point on tooth 43	Tooth	8.00%
18	Bone edge between 43 and 42	Bone	12.00%
19	Vestibular point on tooth 42	Tooth	10.67%
20	Bone edge between 42 and 41	Bone	6.67%
21	Vestibular point on tooth 41	Tooth	12.00%
22	Bone edge between 41 and 31	Bone	5.33%
23	Vestibular point on tooth 31	Tooth	8.00%
24	Bone edge between 31 and 32	Bone	5.33%
25	Vestibular point on tooth 32	Tooth	10.67%
26	Bone edge between 32 and 33	Bone	8.00%
27	Vestibular point on tooth 33	Tooth	14.67%
28	Bone edge between 33 and 34	Bone	9.33%
29	Vestibular point on tooth 34	Tooth	6.67%
30	Bone edge between 34 and 35	Bone	5.33%
31	Vestibular point on tooth 35	Tooth	5.33%
32	Bone edge between 35 and 36	Bone	13.33%
33	Vestibular point on tooth 36	Tooth	17.33%
34	Bone edge between 36 and 37	Bone	2.67%
35	Vestibular point on tooth 37	Tooth	14.67%
36	Bone edge between 37 and 38	Bone	12.00%
37	Vestibular point on tooth 38	Tooth	6.67%
38	Lingual point on tooth 48	Tooth	10.67%
39	Lingual point on tooth 47	Tooth	12.00%
40	Lingual point on tooth 45	Tooth	10.67%
41	Lingual point on tooth 44	Tooth	10.67%
42	Lingual point on tooth 43	Tooth	9.33%
43	Lingual point on tooth 42	Tooth	10.67%
44	Lingual point on tooth 31	Tooth	16.00%
45	Lingual point on tooth 32	Tooth	10.67%
46	Lingual point on tooth 33	Tooth	9.33%
47	Lingual point on tooth 34	Tooth	16.00%
48	Lingual point on tooth 35	Tooth	18.67%
49	Lingual point on tooth 36	Tooth	6.67%
50	Lingual point on tooth 37	Tooth	5.33%
51	Lingual point on tooth 38	Tooth	8.00%
52	48 Distal lingual cusp	Tooth	8.00%
53	<i>48 Mesial lingual cusp</i>	<i>Tooth</i>	<i>37.33%</i>
54	47 Distal lingual cusp	Tooth	9.33%
55	47 Mesial lingual cusp	Tooth	16.00%
56	47 Distal vestibular cusp	Tooth	9.33%
57	47 Mesial vestibular cusp	Tooth	9.33%
58	46 Distal lingual cusp	Tooth	13.33%
59	46 Mesial lingual cups	Tooth	13.33%
60	46 Distal vestibular cusp	Tooth	13.33%
61	46 Mesial vestibular cusp	Tooth	9.33%

Table A1 (continued)

No	Name of the landmark	Location	Point inaccuracy
62	45 Lingual cusp	Tooth	16.00%
63	<i>45 Vestibular cusp</i>	<i>Tooth</i>	<i>44.00%</i>
64	44 Lingual cusp	Tooth	9.33%
65	<i>44 Vestibular cusp</i>	<i>Tooth</i>	<i>40.00%</i>
66	43 cusp	Tooth	50.67%
67	point between incisor edges of 41 and 31	Tooth	22.67%
68	33 cusp	Tooth	25.33%
69	34 Vestibular cusp	Tooth	32.00%
70	34 Lingual cusp	Tooth	17.33%
71	35 Vestibular cusp	Tooth	12.00%
72	35 Lingual cusp	Tooth	13.33%
73	36 Mesial lingual cusp	Tooth	13.33%
74	37 Mesial lingual cusp	Tooth	9.33%
75	38 Mesial lingual cusp	Tooth	14.67%
76	38 Distal lingual cusp	Tooth	78.67%

References

- Automotive Industry Action Group (AIAG): Measurement systems analysis, American society for quality: measurement systems analysis reference manual, 3rd edn; 2002
- Choi JY, Choi JH, Kim NK, Kim Y, Lee JK, Kim MK, et al: Analysis of errors in medical rapid prototyping models. *Int J Oral Maxillofac Surg* 31: 23–32, 2002
- D'haese J, Van De Velde T, Komiyama A, Hultin M, De Bruyn H: Accuracy and complications using computer-designed stereolithographic surgical guides for oral rehabilitation by means of dental implants: a review of the literature. *Clin Implant Dent Relat Res* 14: 321–335, 2012
- Fortin T, Champeboux G, Bianchi S, Buatois H, Coudert J-L: Precision of transfer of preoperative planning for oral implants based on cone-beam CT-scan images through a robotic drilling machine. An in vitro study. *Clin Oral Implants Res* 13: 651–656, 2002
- Ibrahim D, Broilo TL, Heitz C, de Oliveira MG, de Oliveira HW, Nobre SMW, Dos Santos Filho JHG, Silva DN: Dimensional error of selective laser sintering, three-dimensional printing and PolyJet models in the reproduction of mandibular anatomy. *J Craniomaxillofac Surg* 37: 167–173, 2009
- ISO 5725-1: Accuracy (trueness and precision) of measurement methods and results – part 1: general principles and definitions; 1994
- ISO/IEC 17025: General requirements for the competence of testing and calibration laboratories; 2005
- Markowska O, Gardzińska A, Chrzan R: Use of computer tomography and 3DP rapid prototyping technique in cranioplasty planning-analysis of accuracy of bone defect modeling. *Pol J Radiol* 74: 43–46, 2009
- Murugesan K, Anandapandian PA, Sharma SK, Vasantha Kumar M: Comparative evaluation of dimension and surface detail accuracy of models produced by three different rapid prototype techniques. *J Indian Prosthodont Soc* 12: 16–20, 2012
- Nizam A, Gopal RN, Naing L, Hakim AB, Samsudin AR: Dimensional accuracy of the skull models produced by rapid prototyping technology using stereolithography apparatus. *Arch Orolfac Sci* 1: 60–66, 2006
- Olszewski R: Three-dimensional rapid prototyping models in cranio-maxillofacial surgery: systematic review and new clinical applications. *Proc Belgian R Acad Med* 2: 43–77, 2013
- Primo BT, Presotto AC, de Oliveira HW, Gassen HT, Miguens SAQ, Silva AN, et al: Accuracy assessment of prototypes produced using multi-slice and cone-beam computed tomography. *Int J Oral Maxillofac Surg* 41: 1291–1295, 2012
- Salmi M, Paloheimo K-S, Tuomi J, Wolff J, Mäkitie A: Accuracy of medical models made by additive manufacturing (rapid manufacturing). *J Craniomaxillofac Surg* 41: 603–609, 2013
- Silva DN, Gerhardt de Oliveira M, Meurer E, Meurer MI, Lopes da Silva JV, Santa-Bárbara A: Dimensional error in selective laser sintering and 3D-printing of models for craniomaxillary anatomy reconstruction. *J Craniomaxillofac Surg* 36: 443–449, 2008
- Taft RM, Kondor S, Grant GT: Accuracy of rapid prototype models for head and neck reconstruction. *J Prosthet Dent* 106: 399–408, 2011
- Working Group 1 of the Joint Committee for Guides in Metrology (JCGM/WG 1): Evaluation of measurement data—guide to the expression of uncertainty in measurement; 2008